ISSN 1948-9366 (online)

World Journal of

Gastrointestinal Surgery

World J Gastrointest Surg 2021 November 27; 13(11): 1293-1522

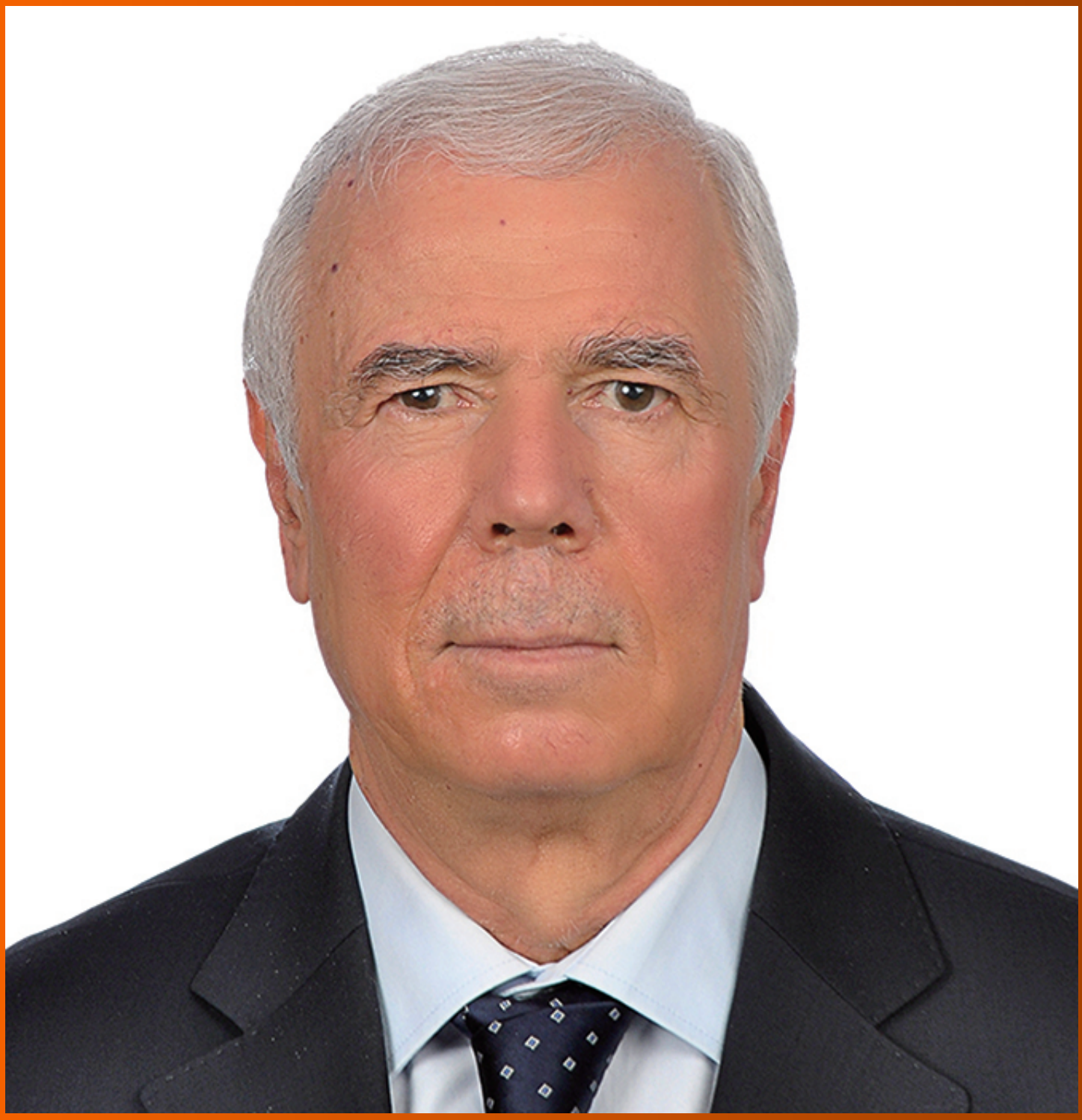

Published by Baishideng Publishing Group Inc

World Journal of Gastrointestinal Surgery

Contents

Monthly Volume 13 Number 11 November 27, 2021

World Journal of Gastrointestinal Surgery

Monthly Volume 13 Number 11 November 27, 2021

Contents

World Journal of Gastrointestinal Surgery

Monthly Volume 13 Number 11 November 27, 2021

Contents

ABOUT COVER

Editorial Board Member of *World Journal of Gastrointestinal Surgery*, Ali Coskun, MD, Associate Professor, Doctor, Department of General Surgery, Izmir Bozyaka Training and Research Hospital, Izmir 35380, Turkey. dralicoskun3564@hotmail.com

AIMS AND SCOPE

The primary aim of *World Journal of Gastrointestinal Surgery* (*WJGS*, *World J Gastrointest Surg*) is to provide scholars and readers from various fields of gastrointestinal surgery with a platform to publish high-quality basic and clinical research articles and communicate their research findings online.

WJGS mainly publishes articles reporting research results and findings obtained in the field of gastrointestinal surgery and covering a wide range of topics including biliary tract surgical procedures, biliopancreatic diversion, colectomy, esophagectomy, esophagostomy, pancreas transplantation, and pancreatectomy, *etc*.

INDEXING/ABSTRACTING

The *WJGS* is now abstracted and indexed in Science Citation Index Expanded (SCIE, also known as SciSearch®), Current Contents/Clinical Medicine, Journal Citation Reports/Science Edition, PubMed, and PubMed Central. The 2021 edition of Journal Citation Reports® cites the 2020 impact factor (IF) for *WJGS* as 2.582; IF without journal self cites: 2.564; 5-year IF: 3.378; Journal Citation Indicator: 0.53; Ranking: 97 among 212 journals in surgery; Quartile category: Q2; Ranking: 73 among 92 journals in gastroenterology and hepatology; and Quartile category: Q4.

RESPONSIBLE EDITORS FOR THIS ISSUE

Production Editor: *Rui-Rui Wu*; **Production Department Director:** *Xiang Li*; **Editorial Office Director:** *Ya-Juan Ma.*

NAME OF JOURNAL
World Journal of Gastrointestinal Surgery

ISSN
ISSN 1948-9366 (online)

LAUNCH DATE
November 30, 2009

FREQUENCY
Monthly

EDITORS-IN-CHIEF
Shu-You Peng, Varut Lohsiriwat, Jin Gu

EDITORIAL BOARD MEMBERS
https://www.wjgnet.com/1948-9366/editorialboard.htm

PUBLICATION DATE
November 27, 2021

INSTRUCTIONS TO AUTHORS
https://www.wjgnet.com/bpg/gerinfo/204

GUIDELINES FOR ETHICS DOCUMENTS
https://www.wjgnet.com/bpg/GerInfo/287

GUIDELINES FOR NON-NATIVE SPEAKERS OF ENGLISH
https://www.wjgnet.com/bpg/gerinfo/240

PUBLICATION ETHICS
https://www.wjgnet.com/bpg/GerInfo/288

PUBLICATION MISCONDUCT
https://www.wjgnet.com/bpg/gerinfo/208

ARTICLE PROCESSING CHARGE
https://www.wjgnet.com/bpg/gerinfo/242

STEPS FOR SUBMITTING MANUSCRIPTS
https://www.wjgnet.com/bpg/GerInfo/239

ONLINE SUBMISSION
https://www.f6publishing.com

World Journal of Gastrointestinal Surgery

Submit a Manuscript: https://www.f6publishing.com

World J Gastrointest Surg 2021 November 27; 13(11): 1448-1462

DOI: 10.4240/wjgs.v13.i11.1448

ISSN 1948-9366 (online)

ORIGINAL ARTICLE

Observational Study

Novel roles of lipopolysaccharide and TLR4/NF-κB signaling pathway in inflammatory response to liver injury in Budd-Chiari syndrome

Jie Li, Xiao-Ming Chen, Chun-Ze Zhou, Wei-Wei Fang, Wei-Fu Lv, De-Lei Cheng

ORCID number: Jie Li 0000-0002-1884-0951; Xiao-Ming Chen 0000-0001-7206-6605; Chun-Ze Zhou 0000-0003-3465-1162; Wei-Wei Fang 0000-0001-8503-0089; Wei-Fu Lv 0000-0002-3681-639X; De-Lei Cheng 0000-0001-6528-1163.

Author contributions: Cheng DL and Lv WF designed the study; Li J, Cheng DL, Zhou CZ, Chen ZM and Fang WW performed the experiments, collected and analyzed the data; Lv WF, Zhou CZ, Chen XM and Fang WW contributed to sample collection and experimental data input into computer; Li J and Cheng DL drafted and wrote the manuscript; Li J and Cheng DL gave advice on the experimental design, interpreted the results and critically revised the manuscript; Lv WF, Zhou CZ and Chen XM provided pathological assistance; all authors read and approved the final version of the manuscript.

Institutional review board statement: All procedures were performed in accordance with the ethical standards of the committee of human experimentation (institutional and national) and with the guidelines of the Helsinki Declaration of 1975 that have been

Jie Li, Chun-Ze Zhou, Wei-Fu Lv, De-Lei Cheng, Department of Interventional Radiology, The First Affiliated Hospital of University of Science and Technology of China, Division of Life Sciences and Medicine, University of Science and Technology of China, Hefei 230001, Anhui Province, China

Xiao-Ming Chen, Department of Gastroenterology, The Second Hospital of Anhui Medical University, Hefei 230000, Anhui Province, China

Wei-Wei Fang, Department of Radiology, The Third People's Hospital of Hefei, Hefei 230022, Anhui Province, China

Corresponding author: De-Lei Cheng, Department of Interventional Radiology, The First Affiliated Hospital of University of Science and Technology of China, Division of Life Sciences and Medicine, University of Science and Technology of China, No. 218 Jixi Road, Hefei 230001, Anhui Province, China. 39055004@qq.com

Abstract

BACKGROUND

Budd-Chiari syndrome (BCS) is an uncommon disorder characterized by obstruction of hepatic venous outflow. To date, the exact mechanism underlying hepatic injury derived from the hepatic venous outflow obstruction in BCS remains largely unknown.

AIM

To assess the role of NF-κB-mediated inflammation in BCS-induced liver injury in humans and rats.

METHODS

A total of 180 rats were randomly assigned into nine groups, including four BCS model groups (1, 3, 6 and 12 wk), four sham-operated groups (1, 3, 6 and 12 wk), and a control group. Lipopolysaccharide (LPS) levels in each group were detected by the Tachypleus Amebocyte Lysate assay. The mRNA and protein levels of TLR4, NF-κB, tumor necrosis factor (TNF)-α, interleukin (IL)-2 and interferon (IFN)-γ were quantified. In addition, 60 patients with BCS and 30 healthy controls were enrolled, and their blood samples were analyzed.

RESULTS

Hepatic and plasma LPS levels were significantly increased in rats. The mRNA and protein expression levels of TLR4, NF-κB and inflammatory cytokines (TNF-α, IL-2 and IFN-γ) in liver tissues were significantly higher in the BCS model groups compared with the other two groups. In addition, the model groups (1, 3, 6 and 12 wk after BCS induction) showed significant differences in the levels of LPS, TLR4, NF-κB, TNF-α, IL-2 and IFN-γ. Notably, there was a significant correlation between the LPS concentrations and mRNA and protein levels of TLR4, NF-κB and inflammatory cytokines. Importantly, it was revealed that the levels of LPS, TLR4, NF-κB and inflammatory cytokines were significantly greater in chronic BCS patients than healthy controls and acute BCS patients.

CONCLUSION

LPS level is markedly elevated in BCS, in turn activating the TLR4/NF-κB signaling pathway, leading to induction of inflammatory cytokines (TNF-α, IL-2 and IFN-γ) in response to BCS-induced liver injury.

Key Words: Budd-Chiari syndrome; Liver injury; Lipopolysaccharide; Nuclear factor-kappa B; Toll-like receptor 4

Core Tip: Budd-Chiari syndrome (BCS) is an uncommon disorder characterized by obstruction of hepatic venous outflow. When the liver becomes congested and damaged, liver fibrosis and cirrhosis can occur. We explored the mechanism involving NF-κB in BCS-induced liver injury in humans and animal models. Results suggest that LPS level is markedly elevated in BCS, and in turn it activates the TLR4/NF-κB signaling pathway, leading to induction of inflammatory cytokines (tumor necrosis factor-α, interleukin-2 and interferon-γ) in response to BCS-induced liver injury. Importantly, our novel findings indicated that the TLR4/NF-κB signaling pathway could be a potential therapeutic target.

Citation: Li J, Chen XM, Zhou CZ, Fang WW, Lv WF, Cheng DL. Novel roles of lipopolysaccharide and TLR4/NF-κB signaling pathway in inflammatory response to liver injury in Budd-Chiari syndrome. *World J Gastrointest Surg* 2021; 13(11): 1448-1462
URL: https://www.wjgnet.com/1948-9366/full/v13/i11/1448.htm
DOI: https://dx.doi.org/10.4240/wjgs.v13.i11.1448

INTRODUCTION

Budd-Chiari syndrome (BCS) is a clinical condition caused by the outflow tract obstruction of the hepatic vein (HV)[1-5]. The primary cause of BCS includes portal vein thrombosis or HV obstruction, while secondary BCS may occur with parasite infection, abscess, cyst, or benign or malignant tumors[1-6]. It has been demonstrated that liver injury is induced by HV outflow tract occlusion in BCS regardless of the etiological factors. However, to date, the exact mechanism underlying BCS-induced hepatic injury remains elusive[6,7].

Previous studies have shown that NF-κB, consisting of two subunits (p50 and p65 heterodimers), plays a pivotal role in the inflammatory response to external stimuli [*e.g.*, lipopolysaccharide (LPS), reactive oxygen species (ROS), tumor necrosis factor (TNF)-α, and interleukin (IL)-2][8-13]. In the NF-κB signaling pathway, the NF-κB heterodimers are phosphorylated by NF-κB (IκB) inhibitor mediated by the IκB kinase (IKK)[8-13]. This activation can result in transportation of activated NF-κB (p50 and p65 heterodimers) from the cytoplasm to the nucleus, and triggers the expression of target genes, generating and releasing inflammatory cytokines, such as TNF-α, IL-2 and interferon (IFN)-γ. Additionally, these inflammatory cytokines can promote the activation of NF-κB, which in turn can mediate a cascade of inflammatory reactions to inflammatory injury.

revised in 2008 (5).

Informed consent statement: All study participants, or their legal guardian, provided informed written consent prior to study enrollment.

Conflict-of-interest statement: The authors declare no conflicts of interest.

Data sharing statement: Data are available on reasonable request from the corresponding author.

STROBE statement: The authors have read the STROBE Statement-checklist of items, and the manuscript was prepared and revised according to the STROBE Statement-checklist of items.

Supported by Natural Science Foundation Project of Anhui Province, No. 1708085QH218.

Country/Territory of origin: China

Specialty type: Gastroenterology and hepatology

Provenance and peer review: Unsolicited article; Externally peer reviewed.

Peer-review report's scientific quality classification

Grade A (Excellent): 0
Grade B (Very good): 0
Grade C (Good): C
Grade D (Fair): 0
Grade E (Poor): 0

Received: January 13, 2021

Peer-review started: January 13, 2021
First decision: July 14, 2021
Revised: August 19, 2021
Accepted: October 31, 2021
Article in press: October 31, 2021
Published online: November 27, 2021

P-Reviewer: Manesis EK
S-Editor: Gao CC
L-Editor: Kerr C
P-Editor: Gao CC

NF-κB-dependent inflammatory responses are involved in the regulation of liver injury due to a variety of factors, including hepatitis virus, poisoning, alcohol and cholestasis[14,15]. Importantly, portal hypertension and imbalance of intestinal flora in BCS can lead to intestinal congestion and edema, as well as increased levels of LPS in the liver. In addition, the congested liver leads to a decrease in blood flow, and thus, LPS is further accumulated. We hypothesized that accumulation of LPS can activate the TLR4/NF-κB signaling pathway through combination of TLR4 in hepatic cells, thereby regulating NF-κB-dependent liver acute and chronic inflammatory damage. To date, however, no relevant research has been carried out[16-18].

In this study, we investigated whether LPS and the LPS-activated TLR4/NF-κB signaling pathway could be involved in the inflammatory response to BCS-induced liver injury in a rat model of BCS and human patients with BCS. The results may assist researchers to better understand the mechanism of the hepatic injury caused by BCS.

MATERIALS AND METHODS

Reagents

Chloroform was purchased from Shanghai Suyi Chemical Reagent Co. Ltd. (Shanghai, China) and Limulus reagent was obtained from Xiamen Limulus Reagent Experimental Factory Co. Ltd. (Xiamen, China). Goat anti-mouse and goat anti-rabbit IgG, as well as phosphate-buffered saline were purchased from Beijing Zhongshan Golden Bridge Biotechnology Co. Ltd. (ZSbio) (Beijing, China). Tween-20 was obtained from Beijing Solarbio Science & Technology Co. Ltd. (Beijing, China).

Induction of BCS in the experimental animals

Male Sprague-Dawley rats (n = 180; body weight, 205-260 g) were used. All animals were housed in individual cages and maintained at room temperature (15-25 °C), with a humidity of 50%-60%. Food and water were given *ad libitum*. The rats were fasted for 12 h before operation and were anesthetized by intraperitoneal injection of 10% chloral hydrate (3 mL/kg). The rats were randomly divided into nine groups of 20 rats each, including four model-based groups (1, 3, 6 and 12 wk after surgical induction of BCS), four sham-operated groups (1, 3, 6 and 12 wk following sham operation), and one control group. Rats in the model groups underwent the following surgical procedures to induce BCS: The retro hepatic inferior vena cava (IVC) was exposed, the tissues surrounding the IVC were dissociated, the 4F catheter was paralleled to the IVC, and the IVC and the catheter were tightly fastened using No. 0 suture, followed by pulling the catheter out and closing the abdomen (Supplementary Figure 1). Penicillin (20 U/rat) was injected intramuscularly after 5 d. In the sham-operated groups, the tissues surrounding the IVC were separated, while they were not ligated. Rats in the control group were fed for 6 wk without any other interventions.

The study protocol was approved by the Ethics Committee of the First Affiliated Hospital of University of Science and Technology of China (Hefei, China; approval No. 2020-N(H)-094).

Digital subtraction angiography of rats

Digital subtraction angiography (DSA) was performed in all rats. On the day before rats were killed, they were anesthetized intraperitoneally with 10% chloral hydrate (3 mL/kg). The skin was incised on either side of the groin to expose the femoral vein. The skin was punctured with a 24G intravenous needle and iodixanol (Jiangsu Hengrui Pharmaceutical Co. Ltd., Nanjing, China) was injected through an intravenous indwelling needle at a flow rate of 1 mL/s with a total volume of 2.5 mL. DSA was performed to visualize the blood flow of the HV and IVC, as well as the formation of IVC occlusion and collateral circulation.

Collection of liver tissues from the experimental rats

According to the random number table method, 12 rats were killed at various time points after treatment. The left lobe of the liver tissue was fixed with 10% formalin and Bouin's solution for histopathological examination.

Measurements of hepatic and plasma LPS levels in rats

Hepatic or plasma LPS levels were determined in the experimental rats. The standard curve was plotted *via* increasing LPS levels: 0.1, 0.25, 0.5 and 1.0 EU/mL solutions. For measurement of LPS levels, 100 μL LPS standards or samples (or rat liver homogenate

solution, or plasma) were added to the non-pyrogen tube, and 100 μL Limulus amebocyte lysate solution was added, gently and evenly shaken, and incubated in a 37 °C incubator for 10 min. After that, they were mixed well with 100 μL chromogenic substrate solution and incubated for 6 min in a 37 °C incubator. At the end of incubation, we added 500 μL azo reagent 1, 2 and 3 solutions in sequence, shaking gently each time until fully mixed, waited for 5 min, and recorded the optical density at 545 nm. The absorbance of the rat liver homogenate sample was substituted into the standard curve, and the sample concentration was calculated, and was multiplied by the dilution multiple to obtain LPS level.

Real-time polymerase chain reaction measurement of β-actin, TLR4, NF-κBp65, IL-2, TNF-α and IFN-γ

The liver tissue (50-100 mg) was cut into pieces, ground in liquid nitrogen, and total RNA was isolated using TRIzol reagent (Life Technologies, Carlsbad, CA, United States). The cDNA was obtained by the RevertAid First Strand cDNA Synthesis Kit (Thermo Fisher Scientific, Waltham, MA, United States). Real-time polymerase chain reaction system (Thermo Fisher Scientific) was used, with the following amplification conditions: 95 °C for 2 min, 95 °C for 5 s, and 60 °C for 10 s for 40 cycles. β-Actin was taken as a reference gene, and the relative expression levels were calculated using the $2^{-\Delta\Delta CT}$ method. The primers used were synthesized by Shanghai Shenggong Bioengineering Co. Ltd. (Shanghai, China), and are summarized in Table 1. All experiments were carried out on three rats.

Western blotting for detection of protein levels of β-actin, TLR4, NF-κBp65, IL-2, TNF-α and IFN-γ

Western blotting was performed to detect the protein levels. In brief, 100 mg liver tissue was extracted and lysed with 1 mL radio-immunoprecipitation assay lysis buffer (Beyotime Institute of Biotechnology, Shanghai, China). The supernatant containing total protein of rat liver tissue was collected after centrifugation at 12000 rpm for 15 min at 4 °C. Protein concentrations were measured using the BCA method. Proteins (30 μg) were separated *via* 10% SDS-PAGE and electrophoretically transferred to equilibrated polyvinylidene difluoride membranes (Millipore, Burlington, MA, United States). After being blocked, the membranes were incubated overnight at 4 °C with the following primary antibodies: TLR4 (1:300; ZSbio), NF-κB (1:300; ZSbio), TNF-α (1:300; ZSbio), IL-2 (1:300; ZSbio), IFN-γ (1:300; ZSbio), and β-actin (Santa Cruz Biotechnology, Dallas, TX, United States). Bound primary antibody was detected by incubation with horseradish-peroxidase-conjugated secondary antibody for 2 h. The protein was detected by an enhanced chemiluminescent kit (Thermo Fisher Scientific), and the ImageJ software (National Institutes of Health, Bethesda, MD, United States) was used for image processing.

Histopathological examination

The liver tissues of rats were fixed in formaldehyde and Bouin's solution, embedded in paraffin and sectioned. According to the standard procedure, liver sections were subjected to hematoxylin-eosin (HE) staining and Masson's trichrome staining, dehydrated, sealed, and images of sections were visualized using a microscope.

Human subjects and detection of LPS levels and key molecules in the TLR4/NF-κB signaling pathway

A total of 60 patients with acute or chronic BCS were enrolled from the First Affiliated Hospital of the University of Science and Technology of China (Hefei, China) from January 2018 to December 2019. The inclusion criteria for acute BCS were as follows: (1) BCS patients with the disease course < 3 mo; (2) Diagnosed with BCS for the first time; (3) No history of alcohol abuse and toxic exposure; and (4) No history of pulmonary heart disease, viral hepatitis, immune hepatitis, or other related diseases. The chronic BCS group included patients with disease course > 3 mo, and with other inclusion criteria similar to the acute BCS group. We also enrolled 30 healthy volunteers as controls.

Blood samples (8 mL) were collected from the cubital veins of the human subjects for subsequent analysis. Then, 3-mL blood samples were anticoagulated with 2% EDTA and were used for measurement of TLR4, in which the positive expression rate of TLR4 in monocytes of each subject was detected by flow cytometry. Next, 3 mL heparin was used for preparation of plasma to detect LPS level in BSC patients. Afterwards, 2 mL non-anticoagulated blood samples was used for preparation of

Table 1 Primers used in this study

	Forward	Reverse
β-actin (150 bp)	5′-CCCATCTATGAGGGTTACGC-3′	5′-TTTAATGTCACGCACGATTTC-3′
TLR4 (186 bp)	5′-GCCGGAAAGTTATTGTGGTGGT-3′	5′-ATGGGTTTTAGGCGCAGAGTTT-3′
NF-κB p65 (108 bp)	5′-AAGATCTGCCGAGTAAACCG-3	5′-TCCCGTGAAATACACCTCAA-3′
IL-2 (113 bp)	5′-CAAGCAGGCCACAGAATTGA-3′	5′-TTCCAGCGTCTTCCAAGTGA-3′
TNF-α (89 bp)	5′-AGGAGGGAGAACAGCAACTC-3′	5′-TGTATGAGAGGGACGGAACC-3′
IFN-γ (130 bp)	5′-CAGGCCATCAGCAACAACAT-3′	5′-GCTGGATCTGTGGGTTGTTC-3′

TLR4: Toll-like receptor 4; NF-κB: Nuclear factor-κB; TNF-α: Tumor necrosis factor-α; IL-2: Interleukin-2; IFN-γ: Interferon-γ.

serum after centrifugation at 1000 rpm for 10 min to detect the levels of NF-κB, IL-2, TNF-α and IFN-γ in BSC patients by commercial ELISA kits (Shanghai Baiwo Technology Co. Ltd., Shanghai, China).

Statistical analysis

Statistical analysis was performed with SPSS 22.0 software (IBM, Armonk, NY, United States). All data were normally distributed and they were expressed as mean ± SD. Comparisons among three groups were performed by one-way analysis of variance (ANOVA). Comparisons between two groups (model and sham-operated groups) was carried out by two-way ANOVA, while the follow-up analysis was conducted by the least significant difference test. Pearson's correlation analysis was used to analyze the correlation among different factors. $P < 0.05$ was considered statistically significant.

RESULTS

Induction of BCS by surgical procedure for HV outflow obstruction in rats

To investigate the mechanism for inflammatory response to liver injury derived from HV outflow obstruction in BCS patients, we initially established a rat model of BCS. The induction of BCS was confirmed by DSA. In the control and sham-operated groups, all rats presented no signs of vascular occlusive disease (*e.g.*, stenosis and occlusion) and collateral angiogenesis of IVC (Figure 1A1 and A2). In the model groups, all rats had HV outflow obstruction caused by IVC obstruction, in which ligation of the IVC above the HV opening was found in 35 rats (72.9%, 35/48), with a coronary lumen stenosis rate of > 85%. In the other 13 rats (17.1%, 13/48), the IVC above the HV opening was fully occluded. In each model group, the formation of collateral circulation in the rat model gradually increased and thickened, with the order of effects as follows: 12 wk > 6 wk > 3 wk > 1 wk after BCS induction (Figure 1A3-A6).

Histopathological analysis revealed that there was no formation of ascites in the model group after 1 wk of BCS induction, and degrees of abdominal effusion were elevated in other model groups at 3, 6 and 12 wk after BCS induction. It was noted that there were no significant changes in the liver tissues in the model group at 1 wk, while different degrees of congestion and enlargement were observed in other model groups at 3, 6 and 12 wk. The HE and Masson's trichrome staining methods confirmed that the liver injury and liver fibrosis showed a gradually aggravating trend, with the most significant effects in the model group at 12 wk. Histopathological findings exhibited no significant difference in liver sections of rats in the sham-operated and the control groups (Figure 1B and Supplementary Figure 2).

Hepatic and plasma levels of LPS in rats with BSC

LPS levels in the liver and plasma samples were calculated by using the standard curve of LPS. The LPS levels in the model group at 1, 3, 6 and 12 wk were 1.16 ± 0.08, 1.80 ± 0.10, 1.31 ± 0.09, and 1.23 ± 0.10 ng/mL, respectively, which were significantly higher than those in the sham-operated groups (0.87 ± 0.07, 0.86 ± 0.06, 0.85 ± 0.07 and 0.85 ± 0.09 ng/mL), and the control group (0.86 ± 0.08 ng/mL). However, there were no significant differences in LPS levels between the control and sham-operated groups. There were significant differences between each pair of model groups. The LPS levels

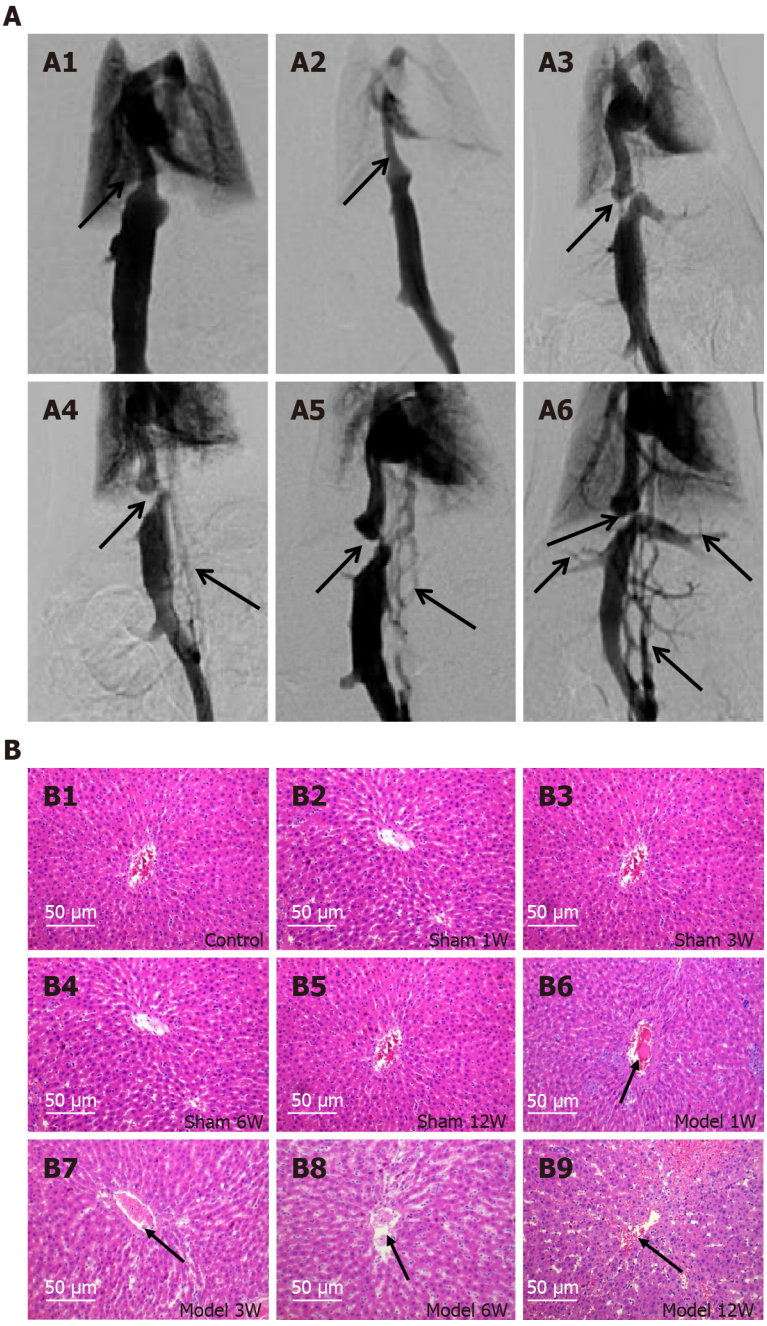

Figure 1 Digital subtraction angiography images and hematoxylin-eosin staining images in the rat model of Budd-Chiari syndrome. A: A1: Control group; A2: The sham operation group. Two groups showed that the inferior vena cava (IVC) blood flow was smooth, but no stenosis or occlusion of the IVC and hepatic vein (HV) (black arrow); A3: In the 1 model group 1W, IVC stenosis above the opening of the HV could be seen, and the contrast agent passed through in a line, without obvious collateral vessel formation (black arrow); A4: In the model group 3W, a small amount of collateral vessel formation around the IVC (black arrow); A5: In the model group 6W, a large number of collateral vessels around the IVC (black arrow); A6: In the model group 12W, the collateral vessels around the IVC were further increased and thickened (black arrow); B: B1: Control group; B2-B5: Four groups of sham operation group, 1W (B2), 3W (B3), 6W (B4) and 12W (B5). Hepatocytes were arranged in a single row radially centered on the central vein, with no change in hepatocytes and hepatic sinusoids (B1–B5); B6: Model group 1W. Hyaline degeneration of rat hepatocytes and no obvious dilation and stagnation of red blood cells in hepatic sinusoids (black arrow); B7: Model group 3W. The hyaline degeneration of rat hepatocytes was aggravated, the hepatocytes around the central vein were necrotic, and the hepatic sinusoids were dilated with a small amount of stasis red blood cells (black arrow); B8: Model group 6W. Large sheet necrosis of liver cells around the central vein, further expansion of liver sinusoids, more stasis of red blood cells in the expanded liver sinusoids (black arrow); B9: Model group 12W. The arrangement of liver cells was disordered, the normal hepatocyte cord disappeared, the hepatic sinusoids were significantly expanded and there was a large number of erythrocytes (black arrow). Original magnification × 200. Bar = 50 μm.

reached the peak in the model group at 3 wk after BCS induction, and then decreased progressively, while it remained higher than that in the control and sham-operated groups until 12 wk, and the difference was significant (Figure 2A).

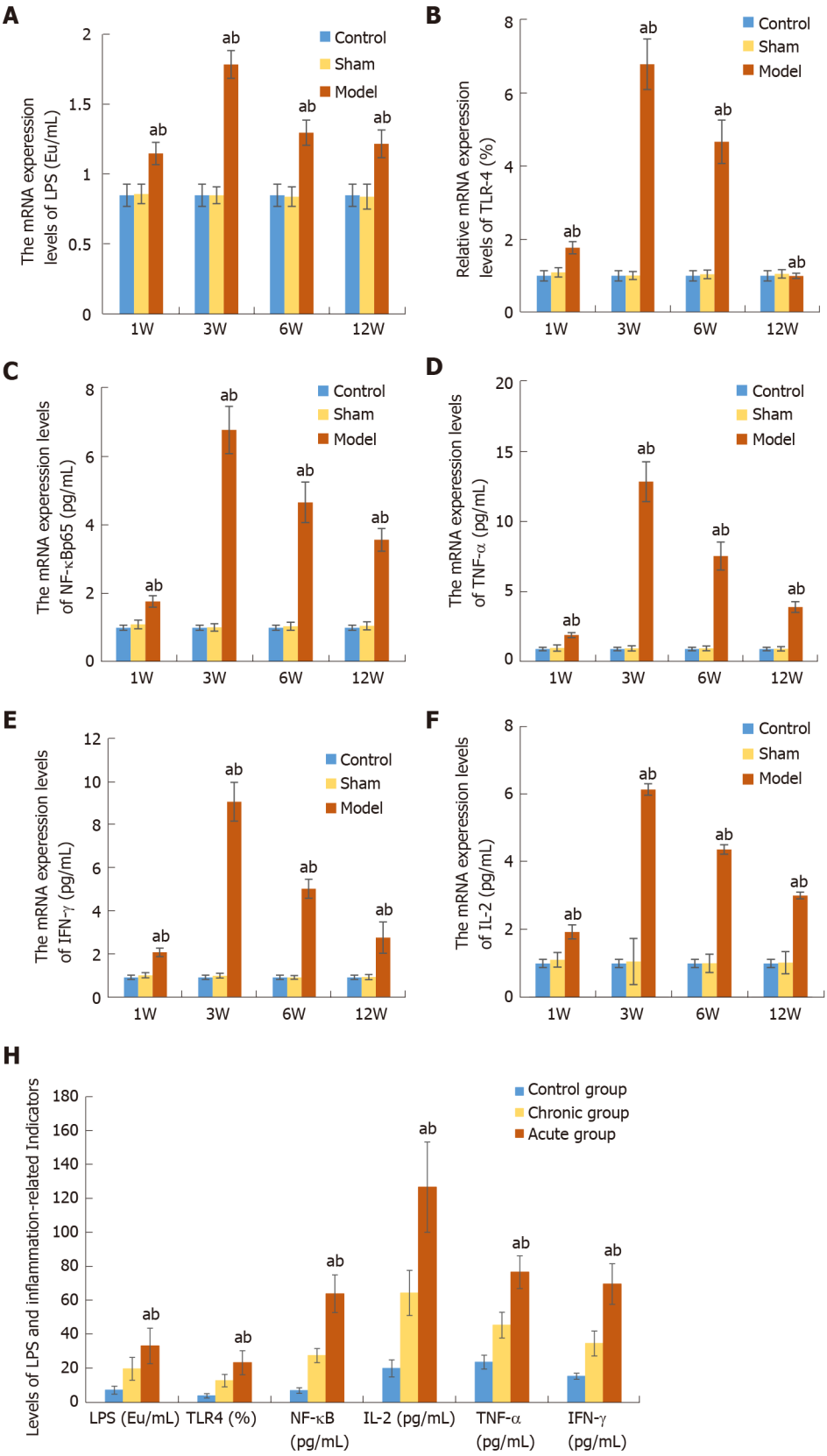
A
The mRNA expression levels of LPS (Eu/mL)
Control
Sham
Model
ab
1W
3W
6W
12W
B
Relative mRNA expression levels of TLR-4 (%)
C
The mRNA expression levels of NF-κBp65 (pg/mL)
D
The mRNA expression levels of TNF-α (pg/mL)
E
The mRNA expression levels of IFN-γ (pg/mL)
F
The mRNA expression levels of IL-2 (pg/mL)
H
Levels of LPS and inflammation-related Indicators
Control group
Chronic group
Acute group
LPS (Eu/mL)
TLR4 (%)
NF-κB (pg/mL)
IL-2 (pg/mL)
TNF-α (pg/mL)
IFN-γ (pg/mL)

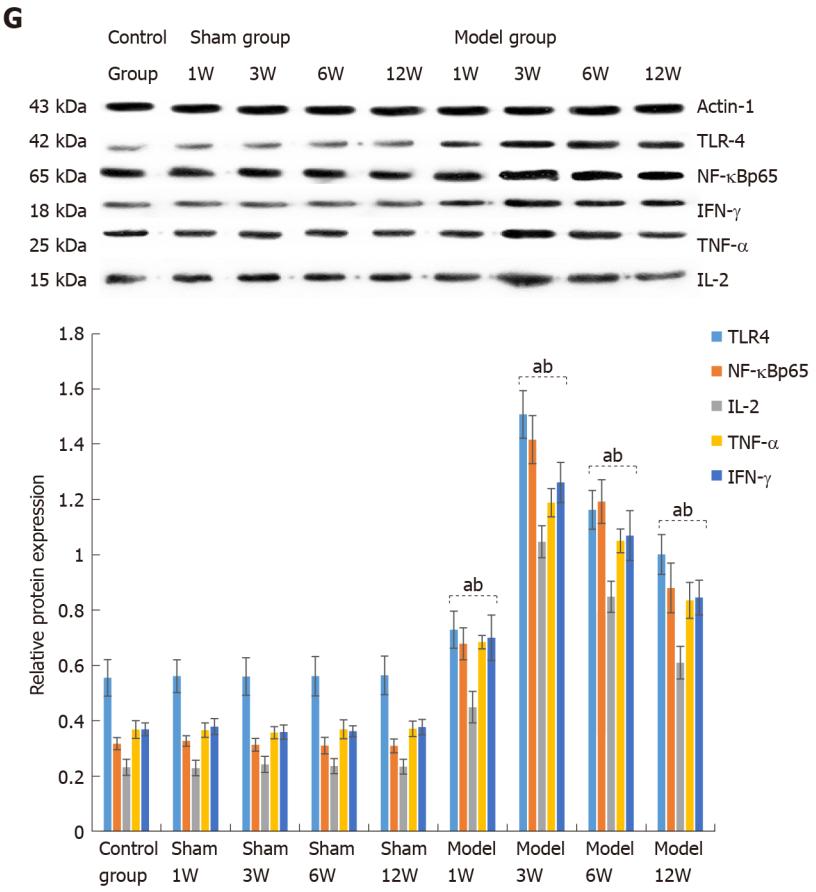

Figure 2 Hepatic mRNA and protein expression levels of lipopolysaccharide and various factors in rats and humans. A: The expression levels of lipopolysaccharide (LPS) in each group; B: TLR4 expression in each group; C: Nuclear factor-kappa B p65 expression in each group; D: Tumor necrosis factor-α expression in each group; E: Interferon-γ expression in each group; F: Interleukin-2 expression in each group; G: Western blot analysis of protein express levels of various factors in the rat liver tissues; H: Levels of LPS and TLR4/NF-κB mediated inflammation-related indicators in the blood samples from human subjects. LPS: Lipopolysaccharide; TLR4: Toll-like receptor 4; NF-κB: Nuclear factor-kappa B; TNF-α: Tumor necrosis factor-α; IL-2: Interleukin-2; IFN-γ: Interferon-γ. $^{a}P < 0.05$ comparisons between subgroups. $^{b}P < 0.05$ comparisons between model subgroups.

Expression levels of TLR4, NF-κB and inflammatory cytokines in rats with BSC

In comparison with the control and sham-operated groups, the mRNA levels of TLR4, NF-κB, TNF-α, IL-2 and IFN-γ were markedly higher in the model groups. However, there were no significant differences in the expression levels between the control and sham-operated groups, while the expression levels were significantly different between each of the model groups and control and sham-operated groups. In the model groups, the expression levels of TLR4, NF-κB, TNF-α, IL-2 and IFN-γ were gradually elevated in the early stage, which reached a peak at 3 wk, and decreased in the later stages, while it was significantly higher than that in the control and sham-operated groups at 12 wk (Figure 2B-F and Table 2).

Similarly, the protein levels of TLR4, NF-κB, TNF-α, IL-2 and IFN-γ were significantly greater in the model groups than those in the sham-operated and control groups, and there were significant differences among the three groups. The levels of these proteins were significantly higher than the normal ranges and reached a peak at 3 wk after BCS induction (Figure 2G and Table 3).

Correlation between LPS concentrations and levels of TLR4, NF-κB, TNF-α, IL-2 and IFN-γ in rats with BSC

mRNA levels of TLR4, NF-κB, TNF-α, IL-2 and IFN-γ were positively correlated with the corresponding protein synthesis (r = 0.959, 0.947, 0.956, 0.964 and 0.971; $P < 0.001$). The LPS and mRNA levels of TLR4, NF-κB, TNF-α, IL-2 and IFN-γ in the model group were highly positively correlated ($r > 0.90$, $P < 0.001$) (Tables 4 and 5 and Figure 3).

Expression levels of TLR4, NF-κB and inflammatory cytokines in patients with BSC

The main findings of the animal experiments were tested in human subjects. Similarly, we found that the levels of LPS, TLR4, NF-κB, IL-2, TNF-α and IFN-γ were

Table 2 mRNA expression levels of TLR4/NF-κB-mediated inflammation-related indicators

	TLR4	NF-κBp65	IL-2	TNF-α	IFN-γ
Control group	1.004 ± 0.139	1.003 ± 0.074	1.001 ± 0.121	1.001 ± 0.126	1.005 ± 0.101
Sham-operated group					
1W	1.101 ± 0.127	1.101 ± 0.127	1.108 ± 0.206	1.068 ± 0.222	1.102 ± 0.121
3W	1.013 ± 0.109	1.013 ± 0.109	1.061 ± 0.168	1.042 ± 0.181	1.082 ± 0.111
6W	1.045 ± 0.118	1.045 ± 0.118	1.006 ± 0.141	1.047 ± 0.164	1.004 ± 0.084
12W	1.059 ± 0.115	1.059 ± 0.115	1.025 ± 0.097	1.017 ± 0.157	1.019 ± 0.118
Model group					
1W	1.773 ± 0.165[a,b]	1.773 ± 0.165[a,b]	1.935 ± 0.217[a,b]	1.991 ± 0.181[a,b]	2.170 ± 0.195[a,b]
3W	6.789 ± 0.692[a,b]	6.789 ± 0.692[a,b]	6.144 ± 0.681[a,b]	12.931 ± 1.424[a,b]	9.172 ± 0.902[a,b]
6W	4.671 ± 0.593[a,b]	4.671 ± 0.593[a,b]	4.372 ± 0.268[a,b]	7.629 ± 0.999[a,b]	5.131 ± 0.441[a,b]
12W	1.003 ± 0.074[a,b]	3.575 ± 0.334[a,b]	3.011 ± 0.326[a,b]	3.991 ± 0.391[a,b]	2.855 ± 0.732[a,b]
Statistics	333.288	464.025	426.396	555.318	509.268
P value	< 0.0001	< 0.0001	< 0.0001	< 0.0001	< 0.0001

[a]*P* < 0.05, comparisons between subgroups, the differences are statistically significant.
[b]*P* < 0.05, comparisons between model subgroups, the differences are statistically significant.
TLR4: Toll-like receptor 4; NF-κB: Nuclear factor-κB; TNF-α: Tumor necrosis factor-α; IL-2: Interleukin-2; IFN-γ: Interferon-γ.

Table 3 Relative protein expression levels of TLR4/NF-κB-mediated inflammation-related indicators

	TLR4	NF-κBp65	IL-2	TNF-α	IFN-γ
Control group	0.555 ± 0.066	0.317 ± 0.022	0.232 ± 0.029	0.368 ± 0.032	0.369 ± 0.023
Sham-operated group					
1W	0.561 ± 0.059	0.327 ± 0.019	0.229 ± 0.028	0.366 ± 0.026	0.379 ± 0.029
3W	0.560 ± 0.068	0.313 ± 0.023	0.242 ± 0.029	0.357 ± 0.022	0.359 ± 0.026
6W	0.561 ± 0.071	0.310 ± 0.030	0.236 ± 0.027	0.369 ± 0.034	0.362 ± 0.020
12W	0.564 ± 0.070	0.309 ± 0.025	0.234 ± 0.027	0.371 ± 0.028	0.377 ± 0.028
Model group					
1W	0.729 ± 0.067[a,b]	0.678 ± 0.058[a,b]	0.449 ± 0.057[a,b]	0.684 ± 0.024[a,b]	0.700 ± 0.082[a,b]
3W	1.507 ± 0.086[a,b]	1.416 ± 0.087[a,b]	1.047 ± 0.058[a,b]	1.188± 0.051[a,b]	1.261 ± 0.073[a,b]
6W	1.162 ± 0.070[a,b]	1.192 ± 0.079[a,b]	0.848 ± 0.056[a,b]	1.050 ± 0.043[a,b]	1.069 ± 0.090[a,b]
12W	1.001 ± 0.072[a,b]	0.880 ± 0.090[a,b]	0.610 ± 0.059[a,b]	0.835 ± 0.065[a,b]	0.845 ± 0.063[a,b]
Statistics	291.836	711.802	608.214	897.062	488.525
P value	< 0.0001	< 0.0001	< 0.0001	< 0.0001	< 0.0001

[a]*P* < 0.05, comparisons between subgroups, the differences are statistically significant.
[b]*P* < 0.05, comparisons between model subgroups, the differences are statistically significant.
TLR4: Toll-like receptor 4; NF-κB: Nuclear factor-κB; TNF-α: Tumor necrosis factor-α; IL-2: Interleukin-2; IFN-γ: Interferon-γ.

significantly higher in BCS patients compared with those in healthy controls. Comparably, the protein levels of LPS, TLR4, NF-κB, IL-2, TNF-α and IFN-γ in patients with acute BCS were significantly higher than those in patients with chronic BCS (Figure 2H and Table 6).

Table 4 Correlation between lipopolysaccharide and mRNA levels of various inflammation-related indicators

	LPS	TLR4	NF-κBp65	IFN-γ	TNF-α	IL-2
LPS	1	0.959[a]	0.945[a]	0.939[a]	0.942[a]	0.944[a]
NF-κBp65	0.945[a]	0.930[a]	1	0.941[a]	0.954[a]	0.966[a]
IL-2	0.939[a]	0.952[a]	0.941[a]	1	0.982[a]	0.946[a]
TNF-α	0.942[a]	0.953[a]	0.954[a]	0.982[a]	1	0.954[a]
IFN-γ	0.944[a]	0.932[a]	0.966[a]	0.946[a]	0.954[a]	1

[a]$P < 0.01$.

LPS: Lipopolysaccharide; TLR4: Toll-like receptor 4; NF-κB: Nuclear factor-κB; TNF-α: Tumor necrosis factor-α; IL-2: Interleukin-2; IFN-γ: Interferon-γ.

Table 5 Correlation between lipopolysaccharide and protein expression of inflammation-related indicators

	LPS	TLR4	NF-κBp65	IFN-γ	TNF-α	IL-2
LPS	1	0.954[a]	0.929[a]	0.931[a]	0.930[a]	0.936[a]
TLR4	0.954[a]	1	0.915[a]	0.900[a]	0.930[a]	0.910[a]
NF-κBp65	0.929[a]	0.915[a]	1	0.954[a]	0.949[a]	0.961[a]
IFN-γ	0.931[a]	0.900[a]	0.954[a]	1	0.938[a]	0.957[a]
TNF-α	0.930[a]	0.930[a]	0.949[a]	0.938[a]	1	0.954[a]
IL-2	0.936[a]	0.910[a]	0.961[a]	0.957[a]	0.954[a]	1

[a]$P < 0.01$.

LPS: Lipopolysaccharide; TLR4: Toll-like receptor 4; NF-κB: Nuclear factor-κB; TNF-α: Tumor necrosis factor-α; IL-2: Interleukin-2; IFN-γ: Interferon-γ.

Table 6 Levels of lipopolysaccharide and TLR4/NF-κB-mediated inflammation-related indicators in the blood samples from human subjects

	LPS (Eu/mL)	TLR4 (%)	NF-κB (pg/mL)	IL-2 (pg/mL)	TNF-α (pg/mL)	IFN-γ (pg/mL)
Control group	8.42 ± 2.33	5.05 ± 1.29	8.15 ± 1.65	21.19 ± 5.01	24.88 ± 4.07	16.60 ± 1.80
Chronic group	20.96 ± 6.70	14.00 ± 3.67	28.75 ± 4.17	65.62 ± 13.26	46.68 ± 7.55	35.87 ± 7.36
Acute group	34.44 ± 10.45[a,b]	24.55 ± 7.0[a,b]	65.17 ± 11.09[a,b]	127.90 ± 26.57[a,b]	77.88 ± 9.61[a,b]	70.90 ± 11.95[a,b]
F	95.541	132.171	524.000	285.085	384.673	340.340

[a]$P < 0.05$, Acute group *vs* Chronic group, the differences are statistically significant.

[b]$P < 0.05$, Acute group *vs* Control group, the differences are statistically significant.

LPS: Lipopolysaccharide; TLR4: Toll-like receptor 4; NF-κB: Nuclear factor-κB; TNF-α: Tumor necrosis factor-α; IL-2: Interleukin-2; IFN-γ: Interferon-γ.

DISCUSSION

The following novel outcomes can be drawn from the results of the present study: (1) LPS levels were significantly elevated in rats with BCS in and human subjects; (2) The TLR4/NF-κB signaling pathway was activated by LPS as demonstrated by a positive correlation between LPS concentrations and expression levels of TLR4 and NF-κB in rats with BSC and human subjects; and (3) Expression of key inflammatory cytokines, including IL-2, TNF-α and IFN-γ, was positively correlated with LPS concentrations. These findings suggest that the LPS-activated TLR4/NF-κB signaling pathway may play a role, at least in part, in the inflammatory response to BCS-induced liver damage.

A large number of previous studies have confirmed that the inflammatory response mediated by NF-κB is involved in the regulation of liver injury caused by hepatitis viruses, alcohol and poisoning[19-24]. NF-κB has also been shown to play a vital role in regulating the inflammation and liver damage, as well as directly regulating the liver fibrosis[25]. In line with findings of previous studies, the results of the present

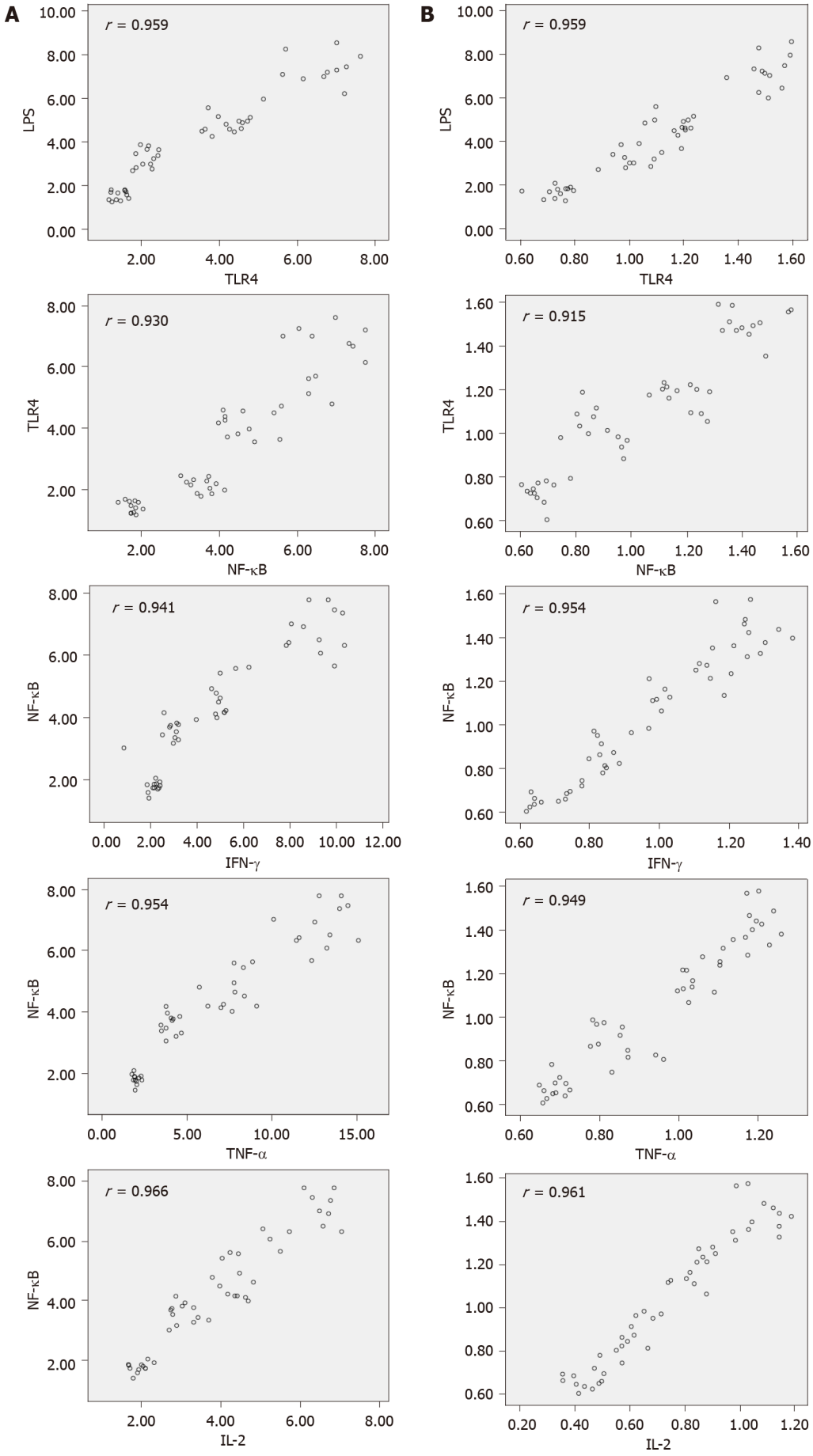

Figure 3 Scatter diagram of lipopolysaccharide and nuclear factor-κB-mediated inflammation-related factors. A: mRNA level; B: Protein level.

LPS: Lipopolysaccharide; TLR4: Toll-like receptor 4; NF-κB: Nuclear factor-κB; TNF-α: Tumor necrosis factor-α; IL-2: Interleukin-2; IFN-γ: Interferon-γ.

study showed that NF-κB mediated inflammation and participated in the BCS-induced liver damage. In an animal model of viral hepatitis and cholestatic liver injury, the level of LPS in the intestine was changed (increased or decreased), and NF-κB was activated through the TLR4 signal transduction pathway to regulate the increase of downstream target gene expression, thereby mediating hepatitis damage or causing delay in the process of liver fibrosis[26,27]. In the current study, expression of LPS, TLR4, NF-κB, TNF-α, IL-2 and IFN-γ in three groups of patients' blood samples and in liver tissues of rats with BCS were significantly higher than those in other groups. The differences in the expression of corresponding indicators between the two groups were significant. In addition, expression levels of hepatic LPS, TLR4, NF-κB, TNF-α, IL-2 and IFN-γ were highly positively correlated at each stage in the BCS animal model (correlation coefficient $r > 0.90$). The results confirmed that the inflammatory response mediated by NF-κB is also involved in the regulation of BCS-induced liver damage. There is a possibility that the increase in NF-κB-mediated inflammation indicators in the liver of BCS rats is associated with IVC obstruction. Under the condition of blocked HV outflow, liver congestion and hypoxia may directly induce NF-κB-mediated inflammation, resulting in liver inflammatory damage. In addition, the obstruction of HV outflow leads to portal hypertension, thereby increasing LPS levels. The accumulated LPS entered the portal venous system, bound to the TLR4 receptor in the liver, activated the TLR4/NF-κB signaling pathway, and induced inflammatory response to BCS-induced liver injury.

The results of this study showed that in the liver tissue of rats with BCS, NF-κB and other inflammatory-related indicators showed an increasing trend in the early stage, reaching a peak at 3 wk, and decreased at a later stage, while it remained significantly higher than other two groups at 12 wk, which showed that the inflammatory reaction mediated by NF-κB not only penetrated the entire course of BCS-associated liver damage, but also caused a different degree of reaction at different periods. The results of DSA also confirmed that the collateral vessels of BCS rats in the 6- and 12-wk groups were significantly more than those in the 1- and 3-wk groups. This finding is also consistent with the indicators of liver damage such as liver transaminase and ascites in patients with acute BCS that are higher than those of chronic BCS patients [7]. However, the liver inflammation-related indicators of BCS rats were still higher than those in the control group at 12 wk, indicating that the autologous collateral formation only relieved the intrahepatic portal hypertension and liver damage to a certain extent, but could not completely resolve the liver congestion and hypoxia, such as the liver inflammatory damage persisted in the HV and IVC, without recanalization by percutaneous transluminal angioplasty.

Our study had some limitations: First, the survival time of experimental rats was limited; therefore, we failed to gain further understanding of the mechanism of liver cirrhosis. Second, the sample size in the rat model groups was small. Percutaneous transluminal angioplasty and intrahepatic portosystemic shunts were not performed, and the NF-κB-mediated inflammatory injury changes in the liver of rats with BCS could not be further studied.

CONCLUSION

This study demonstrated that LPS level becomes markedly elevated in BCS and in turn activates the TLR4/NF-κB signaling pathway. Furthermore, the LPS-activated TLR4/NF-κB signaling pathway may mediate inflammatory response to BCS-induced liver injury. Notably, in the early stage of BCS-induced liver injury, NF-κB-mediated inflammatory response was progressively aggravated, while in the later stage, the inflammatory response was decreased, although it remained abnormally high. These results may assist researchers to better understand the mechanism underlying the BCS-induced hepatic injury. Our novel findings indicated that the LPS-activated TLR4/NF-κB signaling pathway could be a potential target for the development of new treatments for BCS.

ARTICLE HIGHLIGHTS

Research background

Budd-Chiari syndrome (BCS) is an uncommon but potentially life-threatening clinical syndrome of portal and/or inferior vena cava hypertension caused by obstruction of the hepatic and/or inferior vena cava. Liver injury in BCS is considered to be a specific form of liver injury with a mechanism different from that caused by common factors (*e.g.*, viruses, poisoning, alcohol or biliary stasis). Until now, the exact mechanism underlying BCS-induced liver injury is not yet known. It has been shown that lipopolysaccharide (LPS) inactivation is diminished in all causes of liver injury, leading to intrahepatic LPS accumulation, as is the case in acute hepatic injury. LPS accumulation can bind to TLR4 in intrahepatic tissue cells to activate the TLR4/NF-κB pathway and thereby regulate NF-κB-dependent acute and chronic inflammatory liver injury. To date, it remains to be elucidated whether LPS and the TLR4/NF-κB signaling pathway could play a role in the inflammatory response to liver injury in BCS.

Research motivation

We anticipated that investigating the mechanism with involvement of NF-κB may advance our understanding of the pathogenesis of liver injury in BCS, and help to develop new therapeutic strategies for treatment of patients with BCS.

Research objectives

We performed this study, aiming to investigate the potential role of NF-κB-mediated inflammation in BCS-induced liver injury in humans and rats.

Research methods

In this study, 180 rats were randomly assigned into nine groups: four BCS model groups (1, 3, 6 and 12 wk), four sham-operated groups (1, 3, 6 and 12 wk), and one control group. LPS levels in each group were detected by the Tachypleus amebocyte lysate test. The mRNA and protein levels of TLR4, NF-κB, tumor necrosis factor (TNF)-α, interleukin (IL)-2 and interferon (IFN)-γ were quantified. In addition, 60 patients with BCS and 30 healthy controls were enrolled, and their blood samples were analyzed.

Research results

Hepatic and plasma LPS levels were significantly increased in rats. The mRNA and protein expression levels of TLR4, NF-κB and inflammatory cytokines (TNF-α, IL-2 and IFN-γ) in liver tissues were significantly higher in the BCS model groups compared with those in the other two groups. In addition, the model groups (1, 3, 6 and 12 wk after BCS induction) showed significant differences in the levels of LPS, TLR4, NF-κB, TNF-α, IL-2 and IFN-γ. Notably, there was a significant correlation between the LPS concentrations and mRNA and protein levels of TLR4, NF-κB and inflammatory cytokines. Importantly, it was revealed that the levels of LPS, TLR4, NF-κB and inflammatory cytokines were significantly greater in chronic BCS patients than healthy controls and acute BCS patients.

Research conclusions

This study has demonstrated that LPS level is markedly elevated in BCS, in turn activating the TLR4/NF-κB signaling pathway, leading to induction of inflammatory cytokines (TNF-α, IL-2 and IFN-γ) in response to BCS-induced liver injury.

Research perspectives

The findings of the present study implicated that the TLR4/NF-κB signaling pathway could serve as a potential target in the developing of new therapeutic strategies for BCS-induced liver injury, which may ultimately improve the care for patients with BCS.

REFERENCES

1 **Rohringer TJ**, Zaarour C, Williams S, Parra DA. Acute Budd-Chiari syndrome during hepatic vein catheterization. *Radiol Case Rep* 2020; **15**: 1853-1857 [PMID: 32817776 DOI: 10.1016/j.radcr.2020.07.055]

2 **Coilly A**, Potier P, Broué P, Kounis I, Valla D, Hillaire S, Lambert V, Dutheil D, Hernández-Gea V, Plessier A, Vilgrain V, Bureau C. Budd-Chiari syndrome. *Clin Res Hepatol Gastroenterol* 2020; **44**: 420-425 [PMID: 32249150 DOI: 10.1016/j.clinre.2020.03.015]

3 **Valla DC**. Budd-Chiari syndrome/hepatic venous outflow tract obstruction. *Hepatol Int* 2018; **12**: 168-180 [PMID: 28685257 DOI: 10.1007/s12072-017-9810-5]

4 **Ding PX**, Liu C, Han XW, Ding JY, Tse G, Lee EW. Obstructed membranous transformation of the inferior vena cava in patients with hepatic vein-type Budd-Chiari syndrome: A case series. *Clin Res Hepatol Gastroenterol* 2020; **44**: e17-e24 [PMID: 31786160 DOI: 10.1016/j.clinre.2019.10.008]

5 **Shalimar**, Sharma S, Gamanagatti SR, Chauhan A, Vuyyuru SK, Elhence A, Rout G, Saraya A, Gunjan D, Nayak B, Kumar R, Acharya SK. Acute-on-Chronic Liver Failure in Budd-Chiari Syndrome: Profile and Predictors of Outcome. *Dig Dis Sci* 2020; **65**: 2719-2729 [PMID: 31897895 DOI: 10.1007/s10620-019-06005-7]

6 **Hernández-Gea V**, De Gottardi A, Leebeek FWG, Rautou PE, Salem R, Garcia-Pagan JC. Current knowledge in pathophysiology and management of Budd-Chiari syndrome and non-cirrhotic non-tumoral splanchnic vein thrombosis. *J Hepatol* 2019; **71**: 175-199 [PMID: 30822449 DOI: 10.1016/j.jhep.2019.02.015]

7 **Bansal V**, Gupta P, Sinha S, Dhaka N, Kalra N, Vijayvergiya R, Dutta U, Kochhar R. Budd-Chiari syndrome: imaging review. *Br J Radiol* 2018; **91**: 20180441 [PMID: 30004805 DOI: 10.1259/bjr.20180441]

8 **Shim H**, Nam J, Kim SW. NF-κB p65 represses microRNA-124 transcription in diffuse large B-cell lymphoma. *Genes Genomics* 2020; **42**: 543-551 [PMID: 32207045 DOI: 10.1007/s13258-020-00922-y]

9 **Liang H**, Yang X, Liu C, Sun Z, Wang X. Effect of NF-kB signaling pathway on the expression of MIF, TNF-α, IL-6 in the regulation of intervertebral disc degeneration. *J Musculoskelet Neuronal Interact* 2018; **18**: 551-556 [PMID: 30511959]

10 **Afonina IS**, Zhong Z, Karin M, Beyaert R. Limiting inflammation-the negative regulation of NF-κB and the NLRP3 inflammasome. *Nat Immunol* 2017; **18**: 861-869 [PMID: 28722711 DOI: 10.1038/ni.3772]

11 **Wu J**, Ding J, Yang J, Guo X, Zheng Y. MicroRNA Roles in the Nuclear Factor Kappa B Signaling Pathway in Cancer. *Front Immunol* 2018; **9**: 546 [PMID: 29616037 DOI: 10.3389/fimmu.2018.00546]

12 **Jung HJ**, Zhang YL, Kim DK, Rhee CS, Kim DY. The Role of NF-κB in Chronic Rhinosinusitis With Nasal Polyps. *Allergy Asthma Immunol Res* 2019; **11**: 806-817 [PMID: 31552716 DOI: 10.4168/aair.2019.11.6.806]

13 **Ye N**, Wang H, Li Q, Lin C, Huahua F, Lin S, Hong J, Meng C. Activation of PXR inhibits LPS-induced NF-κB activation by increasing IκBα expression in HepG2 cells. *Mol Cell Toxicol* 2018; **14**: 93-104 [DOI: 10.1007/s13273-018-0012-6]

14 **Yang L**, Sun YY, Liu YR, Yin NN, Bu FT, Yu HX, Du XS, Li J, Huang C. PTP1B promotes macrophage activation by regulating the NF-κB pathway in alcoholic liver injury. *Toxicol Lett* 2020; **319**: 11-21 [PMID: 31711802 DOI: 10.1016/j.toxlet.2019.11.001]

15 **Czauderna C**, Castven D, Mahn FL, Marquardt JU. Context-Dependent Role of NF-κB Signaling in Primary Liver Cancer-from Tumor Development to Therapeutic Implications. *Cancers (Basel)* 2019; **11** [PMID: 31349670 DOI: 10.3390/cancers11081053]

16 **Ahmed N**, El-Agamy DS, Mohammed GA, Abo-Haded H, Elkablawy M, Ibrahim SRM. Suppression of LPS-Induced Hepato- and Cardiotoxic Effects by Pulicaria petiolaris *via* NF-κB Dependent Mechanism. *Cardiovasc Toxicol* 2020; **20**: 121-129 [PMID: 31273688 DOI: 10.1007/s12012-019-09539-4]

17 **Xie C**, Yagai T, Luo Y, Liang X, Chen T, Wang Q, Sun D, Zhao J, Ramakrishnan SK, Sun L, Jiang C, Xue X, Tian Y, Krausz KW, Patterson AD, Shah YM, Wu Y, Gonzalez FJ. Activation of intestinal hypoxia-inducible factor 2α during obesity contributes to hepatic steatosis. *Nat Med* 2017; **23**: 1298-1308 [PMID: 29035368 DOI: 10.1038/nm.4412]

18 **Kron P**, Linecker M, Limani P, Schlegel A, Kambakamba P, Lehn JM, Nicolau C, Graf R, Humar B, Clavien PA. Hypoxia-driven Hif2a coordinates mouse liver regeneration by coupling parenchymal growth to vascular expansion. *Hepatology* 2016; **64**: 2198-2209 [PMID: 27628483 DOI: 10.1002/hep.28809]

19 **Wu XQ**, Yang Y, Li WX, Cheng YH, Li XF, Huang C, Meng XM, Wu BM, Liu XH, Zhang L, Lv XW, Li J. Telomerase reverse transcriptase acts in a feedback loop with NF-κB pathway to regulate macrophage polarization in alcoholic liver disease. *Sci Rep* 2016; **6**: 18685 [PMID: 26725521 DOI: 10.1038/srep18685]

20 **Zhou H**, Yu M, Zhao J, Martin BN, Roychowdhury S, McMullen MR, Wang E, Fox PL, Yamasaki S, Nagy LE, Li X. IRAKM-Mincle axis links cell death to inflammation: Pathophysiological implications for chronic alcoholic liver disease. *Hepatology* 2016; **64**: 1978-1993 [PMID: 27628766 DOI: 10.1002/hep.28811]

21 **Song J**, Han X, Yao YL, Li YM, Zhang J, Shao DY, Hou LS, Fan Y, Song SZ, Lian LH, Nan JX, Wu YL. Acanthoic acid suppresses lipin1/2 *via* TLR4 and IRAK4 signalling pathways in EtOH- and lipopolysaccharide-induced hepatic lipogenesis. *J Pharm Pharmacol* 2018; **70**: 393-403 [PMID: 29341132 DOI: 10.1111/jphp.12877]

22 **El-Agamy DS**. Pirfenidone ameliorates concanavalin A-induced hepatitis in mice *via* modulation of reactive oxygen species/nuclear factor kappa B signalling pathways. *J Pharm Pharmacol* 2016; **68**:

1559-1566 [PMID: 27734496 DOI: 10.1111/jphp.12651]

23 **Yoneda M**, Hyun J, Jakubski S, Saito S, Nakajima A, Schiff ER, Thomas E. Hepatitis B Virus and DNA Stimulation Trigger a Rapid Innate Immune Response through NF-κB. *J Immunol* 2016; **197**: 630-643 [PMID: 27288535 DOI: 10.4049/jimmunol.1502677]

24 **Fang ZZ**, Tanaka N, Lu D, Jiang CT, Zhang WH, Zhang C, Du Z, Fu ZW, Gao P, Cao YF, Sun HZ, Zhu ZT, Cai Y, Krausz KW, Yao Z, Gonzalez FJ. Role of the lipid-regulated NF-κB/IL-6/STAT3 axis in alpha-naphthyl isothiocyanate-induced liver injury. *Arch Toxicol* 2017; **91**: 2235-2244 [PMID: 27853831 DOI: 10.1007/s00204-016-1877-6]

25 **Zheng H**, Wang X, Zhang Y, Chen L, Hua L, Xu W. Pien-Tze-Huang ameliorates hepatic fibrosis *via* suppressing NF-κB pathway and promoting HSC apoptosis. *J Ethnopharmacol* 2019; **244**: 111856 [PMID: 30959141 DOI: 10.1016/j.jep.2019.111856]

26 **Qin B**, Wei T, Wang L, Ma N, Tang Q, Liang Y, Yang Z, Zhou L, Zhong R. Decreased expression of TIPE2 contributes to the hyperreactivity of monocyte to Toll-like receptor ligands in primary biliary cirrhosis. *J Gastroenterol Hepatol* 2016; **31**: 1177-1183 [PMID: 26644386 DOI: 10.1111/jgh.13251]

27 **Das D**, Sarkar N, Sengupta I, Pal A, Saha D, Bandopadhyay M, Das C, Narayan J, Singh SP, Chakravarty R. Anti-viral role of toll like receptor 4 in hepatitis B virus infection: An *in vitro* study. *World J Gastroenterol* 2016; **22**: 10341-10352 [PMID: 28058014 DOI: 10.3748/wjg.v22.i47.10341]

Published by **Baishideng Publishing Group Inc**
7041 Koll Center Parkway, Suite 160, Pleasanton, CA 94566, USA
Telephone: +1-925-3991568
E-mail: bpgoffice@wjgnet.com
Help Desk: https://www.f6publishing.com/helpdesk
https://www.wjgnet.com